

Electrical resistivity and magnetic susceptibility roundings above the superconducting transition in $Y_1Ba_2Cu_3O_{7-\delta}$

This article has been downloaded from IOPscience. Please scroll down to see the full text article.

1991 J. Phys.: Condens. Matter 3 5219

(<http://iopscience.iop.org/0953-8984/3/27/017>)

View [the table of contents for this issue](#), or go to the [journal homepage](#) for more

Download details:

IP Address: 171.66.16.147

The article was downloaded on 11/05/2010 at 12:20

Please note that [terms and conditions apply](#).

LETTER TO THE EDITOR

Electrical resistivity and magnetic susceptibility roundings above the superconducting transition in $Y_1Ba_2Cu_3O_{7-\delta}$

Félix Vidal, C Torrón, J A Veira, F Miguélez and J Maza

Laboratorio de Física de Materiales, Departamento de Física de la Materia Condensada, Universidad de Santiago de Compostela, 15706 Spain

Received 24 April 1990

Abstract. We report high-resolution data of the electrical resistivity and of the magnetic susceptibility rounding effects above the superconducting transition in single-phase polycrystalline $YBa_2Cu_3O_{7-\delta}$ compounds. These data may be explained quantitatively and consistently, over two orders of magnitude in reduced temperature, by direct three-dimensional thermodynamic fluctuations of the amplitude of a two-component order parameter in unconventional (non-s-wave pairing) superconductors. The resulting order parameter correlation length amplitudes are $\xi_{ab}(0) = (12 \pm 3) \text{ \AA}$, and $\xi_{\perp}(0) = (1.4 \pm 0.4) \text{ \AA}$, the Lawrence–Doniach effective interlayer distance is $d_c = (8 \pm 2) \text{ \AA}$, and the Ginzburg reduced temperature is $\varepsilon_G = (0.7 \pm 0.3) \times 10^{-2}$.

The aim of this letter is twofold. First, we present high-resolution measurements of the rounding above the superconducting transition of the magnetic susceptibility in the low magnetic field limit, $\chi(T)$, and of the electrical resistivity, $\rho(T)$, in the *same* single phase (to 4%) $Y_1Ba_2Cu_3O_{7-\delta}$ polycrystalline samples ($\delta \leq 0.1$). Although the rounding above the superconducting transition of $\rho(T)$ [1–4] and, *independently*, of $\chi(T)$ [5–7] have been measured in detail by various groups, to our knowledge this is the first time that high resolution data of both observables are obtained in the *same* samples. Due to the influence of non-intrinsic effects (as, for instance, twinning or impurities that may be present even in single-crystal samples, and polycrystallinity in granular samples), measurements in the *same* samples may help to extract and to analyse simultaneously and consistently the *intrinsic* rounding effects in both observables. These experimental results will be compared with other existing high-precision resistivity rounding data [3, 4] and, *independently*, $\Delta\chi_{\perp}^i(T)$ data [5–7] in single-crystal or grain-aligned $Y_1Ba_2Cu_3O_{7-\delta}$ samples. In addition, the intrinsic fluctuation-induced diamagnetism, $\Delta\chi_{\perp}^i(T)$, and the paraconductivity, $\Delta\sigma_{ab}^i(T)$, in the *ab* plane are extracted from these rounding data using the same systematics. Then, and this is the second aim of this letter, these results on $\Delta\chi_{\perp}^i(T)$ and $\Delta\sigma_{ab}^i(T)$ are compared with each other and with the existing theories based on thermodynamic fluctuations of the superconducting order parameter amplitude (SCOPF):

(i) In the mean-field-like region (MFR), the Lawrence and Doniach (LD) [8] extensions to layered materials of the Aslamazov and Larkin (AL) [9] approach for $\Delta\sigma_{ab}^i(T)$ and of the Schmidt (s) approach for $\Delta\chi_{\perp}^i(T)$ [10, 11].

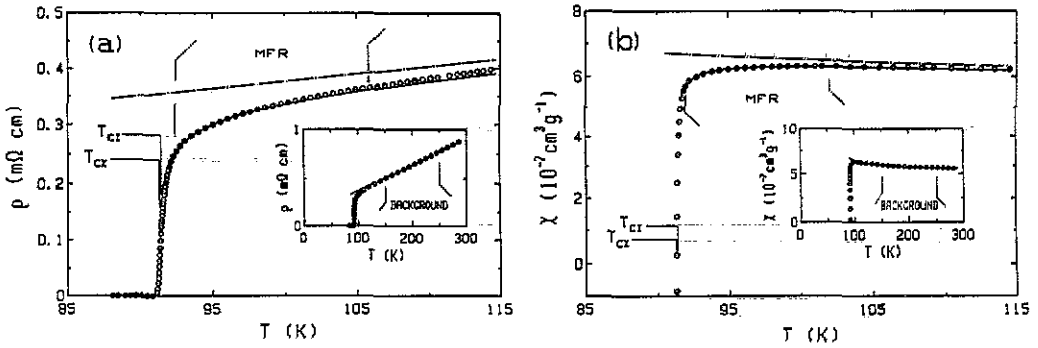


Figure 1. An example of the temperature behaviour of (a) the measured resistivity and (b) of the magnetic susceptibility. The chain lines are the corresponding backgrounds, and the full lines are the mean-field predictions. The mean-field regions in (a) and (b) correspond to, respectively, equations (2) and (3).

(ii) Beyond the MFR, closer to the superconducting transition, the scaling approaches that of various groups [12–14]. Our results strongly suggest that the *direct* SCOPF effects of a two-component ($n = 2$) superconducting order parameter fluctuating in three dimensions (3D) may explain *quantitatively* and *consistently* both $\Delta\sigma'_{ab}(T)$ and $\Delta\chi'_{\perp}(T)$ in $Y_1Ba_2Cu_3O_{7-\delta}$ compounds.

The measurements have been performed on three $Y_1Ba_2Cu_3O_{7-\delta}$ polycrystalline samples having different granularity characteristics. Their preparation, and details of their general structural and stoichiometric properties have been reported in [1] and in references indicated therein. Let us just note here that x-ray diffraction analyses indicate that all samples are single phase to 4%, and $\delta \leq 0.1$. Resistivity was measured by a standard four-probe lock-in method (37 Hz), and the relative resolutions were $1 \mu\Omega \text{ cm}$ and 10 mK for, respectively, $\rho(T)$ and T [1, 2]. Magnetization, $M(T)$, data in the low magnetic field limit ($H \leq 0.3 \text{ T} \ll H_{c2}(0)$) were obtained by using a quantum design (QD) superconducting quantum interferometer device (SQUID) magnetometer. The relative resolutions were 10^{-8} emu for M and 0.1 K for T . Following our previous paraconductivity results [1, 2], this temperature resolution will probably allow one to probe, for the first time with $\chi(T)$, the crossover region beyond the MFR, closer to the superconducting transition than previously possible. Other experimental details as well as the measurement protocol will be presented elsewhere. We just note here that in order to be able to compare quantitatively the $\rho(T)$ and the $\chi(T)$ results, the different thermometers of both the QD system and those used in the $\rho(T)$ measurements were calibrated *together* to better than 0.1 K.

An example of our results on $\rho(T)$ and $\chi(T)$ for the *same* sample is shown in figure 1(a) and (b). These $\chi(T)$ data were obtained with $H = 50 \text{ mT}$. The granular nature of the sample is clearly reflected in these curves. For instance, both the absolute value of $\rho(T)$ and its slope are affected by the reduction of the *effective* cross section in polycrystal samples [1, 2]. Also, due probably to the presence of some paramagnetic impurities and to localized moments originated from oxygen defects [3–5], $\chi(T)$ in the normal region increases somewhat as T decreases. However, these non-intrinsic effects, always present to some extent when analysing critical phenomena in any real (even single-crystal) material, may be easily eliminated by an adequate data analysis. In the case of $\Delta\sigma'(T)$

such a treatment has been detailed in [1] and [2], the only modification made here is the use of a linear temperature dependence for the intrinsic normal (background) resistivity in the ab plane, $\rho_{ab}^i(T)$, instead of the Anderson-Zou (AZ) dependence used in [2]. As we have clearly indicated in [1], the use of either T -dependence *does not* have any important influence on the extracted $\Delta\sigma_{ab}^i(T)$ (see also later). However, recent $\rho_{ab}^i(T)$ data seem to suggest a slightly better adequacy of the linear behaviour [15, 16]. So, in the present work the background resistivity has been obtained by using $\rho_{ab}^i = C_1^i + C_2^i T$, with $C_1^i = 5 \mu\Omega \text{ cm}$ and $C_2^i = 0.5 \mu\Omega \text{ cm K}^{-1}$, which are well within the average values from the data of [3, 4, 15-17]: $C_1^i = (0 \pm 10) \mu\Omega \text{ cm}$ and $C_2^i = (0.5 \pm 0.2) \mu\Omega \text{ cm K}^{-1}$. An example of such a background is the chain line in figure 1(a), and in the inset figure. In this example and concerning equation (1) of [2], the effective cross section parameter (which also takes into account the path lengthening due to the random orientation of the ab plane of the different domains) is $p = 0.19$, whereas the average interdomain resistivity is $\rho_{cl} = 0.09 \text{ m}\Omega \text{ cm}$. The extraction of $\Delta\chi_{\perp}^i(T)$, the intrinsic susceptibility rounding in the ab plane (for H perpendicular to the ab plane), from the measured $\chi(T)$ in granular samples follows similar ideas to those of $\Delta\sigma_{ab}^i(T)$. Noting that as $\Delta\chi_{\perp}^i(T) \gg \Delta\chi_{\parallel}^i(T)$ (H parallel to the ab plane) [5-7, 10, 11], the relationship between $\Delta\chi_{\perp}^i(T)$ and $\chi(T)$ may easily be approximated by

$$\Delta\chi_{\perp}^i(T) \approx 3Z[\chi_B(T) - \chi(T)] \quad (1)$$

where $\chi_B(T)$ is the background susceptibility, Z is the ratio of the nominal density to the sample density, and the factor 3 takes into account the random orientation of the ab planes of each sample domain with respect to the applied magnetic field H . All the non-intrinsic contributions to $\chi(T)$ associated with magnetic impurities and oxygen defects are supposed also to be contained in $\chi_B(T)$, which may then be approximated as [5]: $\chi_B(T) = A/T + BT + C$. These three sample-dependent constants are obtained by fitting $\chi_B(T)$ in the *same* background region as that used for $\rho_B(T)$ [1, 2], i.e., between $T_{cl} + 60 \text{ K}$ ($\approx 150 \text{ K}$) and $T_{cl} + 160 \text{ K}$ ($\approx 250 \text{ K}$). An example of such a background is the chain line in figure 1(b), and in the inset of the figure.

The two other main ingredients in comparing $\Delta\sigma_{ab}^i$ and $\Delta\chi_{\perp}^i$ with theory are the mean-field-like temperature, T_{co} and region (MFR). We have observed that for all the samples studied here, and this is a basic result, T_{cl} , the temperature where $\rho(T)$ around the transition has its inflexion point, agrees to within $\pm\Delta T_{cl}$ with T_{cx} , the latter being defined as the temperature where $\chi(T)$ goes through zero. ΔT_{cl} is the upper half-width of the resistive transition as defined in [1], and it is less than 0.3 K for all the samples studied here. In the examples of figure 1, $T_{cl} = 91.4 \text{ K}$ and $T_{cx} = 91.3 \text{ K}$, whereas $\Delta T_{cl} = 0.22 \text{ K}$. These results strongly suggest, therefore, the adequacy of the choice of T_{cl} or T_{cx} as T_{co} . Furthermore, to avoid the use of elaborated criteria (i.e., that of Ginzburg) that depend on high powers of not well-known parameters in HTSC (for instance, κ^4), the T -location of the MFR may be crudely bounded through $\Delta\rho_{ab}^i(T)/\rho_B^i(T)$ or $\Delta\chi_{\perp}^i(T)/\chi_B^i(T)$, which are related to the relative fluctuation amplitude of the superconducting order parameter [11]. Our previous results on $\Delta\sigma_{ab}^i(T)$ in different HTSC systems [1, 2] clearly indicate that the T -region where the mean-field theory (the LD-like approaches) applies corresponds to $0.1 \approx \Delta\rho_{ab}^i(T)/\rho_B^i(T) \approx 0.4$, or equivalently

$$0.1 \approx \Delta\sigma_{ab}^i(T)/\sigma_B^i(T) \approx 0.6 \quad (2)$$

and also to $10^{-2} \approx \varepsilon \approx 10^{-1}$, where $\varepsilon \equiv \ln T/T_{cl}$, is the reduced temperature. Note that the lower temperature limit agrees qualitatively with that obtained using the Ginzburg criterion [11]. Above the high-temperature limit not only will the Ginzburg-Landau-

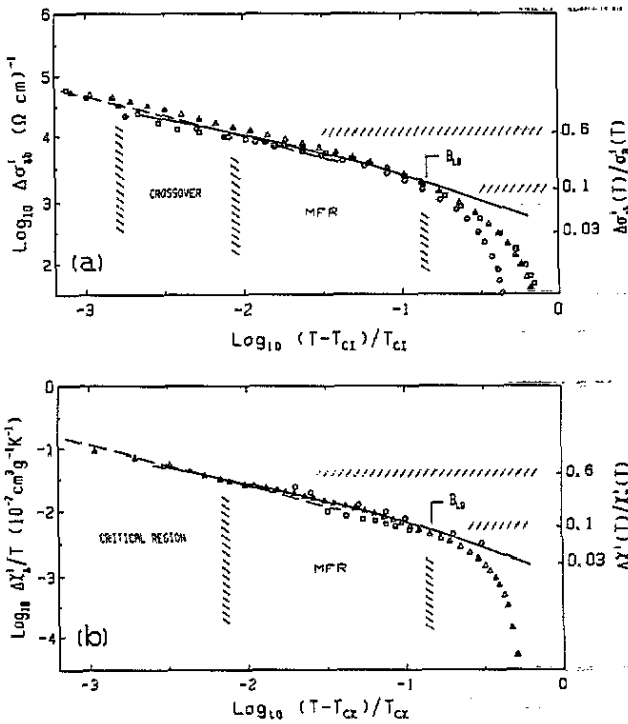


Figure 2. (a) Intrinsic paraconductivity and (b) paramagnetism in the *ab* plane of $Y_1Ba_2Cu_3O_{7-\delta}$ compounds. The full lines were obtained from the Lawrence-Doniach-like extensions of the Aslamazov-Larkin and of the Schmidt mean-field approaches. The broken lines are the scaling predictions beyond the MFR.

like theories probably fail (for instance, the transverse superconducting correlation lengths become smaller than the interatomic distances, see also [11]), but also the uncertainties associated with any data analysis increase considerably. The central result here is that by combining the mean-field theoretical results for $\Delta\sigma_{ab}^i(T)$ and $\Delta\chi_{\perp}^i(T)$ (see below) with our experimental results for $\sigma_B(T)$ and $\chi_B^i(T)$, the above relation leads, for $Y_1Ba_2Cu_3O_{7-\delta}$ samples, to

$$0.1 \approx \Delta\chi_{\perp}^i(T)/\chi_B^i(T) \approx 0.6 \quad (3)$$

which, in addition, we are going to see corresponds to $10^{-2} \approx \varepsilon \approx 10^{-1}$, the ε -region where the mean-field-like theory explains very well $\Delta\chi_{\perp}^i(\varepsilon)$. Moreover, we are going to see here that by using such a lower MFR limit as the Ginzburg reduced temperature, ε_G , we may explain quantitatively the absolute amplitude of $\Delta\sigma_{ab}^i(\varepsilon)$ and $\Delta\chi_{\perp}^i(\varepsilon)/T$ in the crossover region. These findings strongly support the above proposal for the T -location of the MFR in YBCO materials.

The intrinsic $\Delta\sigma_{ab}^i(\varepsilon)$ and $\Delta\chi_{\perp}^i(\varepsilon)/T$ for $Y_1Ba_2Cu_3O_{7-\delta}$ superconductors in the *ab* plane, extracted from the $\rho(T)$ and $\chi(T)$ data as indicated above, are represented in, respectively, figure 2(a) and (b). The triangles have been obtained from the corresponding data of figure 1. Circles and squares in figure 2(a) correspond to the resistivity in the *ab* plane of two single-crystals measured, respectively, by Friedmann and coworkers [3] and Hikita and Suzuki [4]. The $\Delta\sigma_{ab}^i(\varepsilon)$ data extracted from the other

granular samples studied here and in [1], which have very different long-scale structural inhomogeneities, are well within the data dispersion of figure 2. The comparison of figure 2(a) with figure 1 of [2] clearly shows that, as first pointed out in [1], the use of an AZ or a linear background leads to $\Delta\sigma_{ab}^i(\varepsilon)$ values that agree with each other to within the data dispersion. This is because, when analysing critical phenomena, the detailed functional form of the background should not have any important influence on the critical contribution, provided a high-quality fitting in a wide background region is realized [18]. Circles and squares in figure 2(b) correspond to $\Delta\chi_{\perp}^i(\varepsilon)$ data obtained by, respectively, Johnston and coworkers in a grain-aligned $Y_1Ba_2Cu_3O_{7-\delta}$ sample [6] and by Kanoda and coworkers in a polycrystal sample [5]. Again, this time for $\Delta\chi_{\perp}^i(\varepsilon)$, a good agreement is found between these two different results, although the data of [5] and [6] penetrate only up to $T - T_{co} \geq 2$ K, i.e., an order of magnitude less in reduced temperature than our data. A remarkable and new result of figure 2(a) and (b) is the very similar (at a quantitative level) reduced-temperature behaviour of both observables through three orders of magnitude in ε .

The above results, including the amplitude of both observables, may be easily understood in terms of the existing theoretical approaches for *direct* SCOPF effects in layered superconductors. In the MFR, the Lawrence–Doniach-like approaches predict [8–11, 19, 20]:

$$\Delta\sigma_{ab}^i(\varepsilon) = (A_{AL}/\varepsilon)(1 + B_{LD}/\varepsilon)^{-1/2} \quad (4)$$

and

$$\Delta\chi_{\perp}^i(\varepsilon)/T = (A_S/\varepsilon)(1 + B_{LD}/\varepsilon)^{-1/2} \quad (5)$$

where the Aslamazov–Larkin amplitude for unconventional (non-s-wave pairing) superconductors is given by [19], $A_{AL} = ne^2/16\hbar d_e$, and where we have assumed a pair-breaking factor $r = 1$ (see also [2]). The 2D–3D Lawrence–Doniach crossover coefficient is given by [8], $B_{LD} = (2\xi_{\perp}(0)/d_e)^2$, and the Schmidt amplitude is given by [11], $A_S = \pi k_B \varphi_0^{-2} \xi_{ab}^2/3d_e$. In these expressions, n is the number of components of the order parameter, e is the electron charge, \hbar is the reduced Plank constant, d_e is the *effective* interlayer distance (which takes into account the double periodicity of these compounds [19]), k_B is the Boltzmann constant, φ_0 is the flux quantum and $\xi_{ab}(0)$ and $\xi_{\perp}(0)$ are the amplitudes of the superconducting correlation length in the *ab* plane and, respectively, perpendicular to this plane. Note that (in cgs units) $A_S/A_{AL} = 2.47 \times 10^{-10} \xi_{ab}(0)^2/n$, which is independent of d_e .

For $\varepsilon \ll B_{LD}$, the above equations reduce to their 3D limit ($\xi_{\perp}(\varepsilon) \gg d_e$)

$$\Delta\sigma_{ab}^i(\varepsilon) = A_{AL}(3D)\xi_{ab}(\varepsilon) \quad (6)$$

and

$$\Delta\chi_{\perp}^i(\varepsilon)/T = A_S(3D)\xi_{ab}(\varepsilon) \quad (7)$$

where $A_{AL}(3D) = ne^2/32\hbar\xi_{ab}(0)\xi_{\perp}(0)$, $A_S(3D) = \pi k_B \varphi_0^{-2} \xi_{ab}(0)/6\xi_{\perp}(0)$ and $\xi_{ab}(\varepsilon) = \xi_{ab}(0)\varepsilon^{-1/2}$. The important point here is that beyond the MFR, closer to T_{co} , (6) and (7) may still be a good approximation if an adequate Ginzburg–Landau correlation length, $\xi_{ab}(\varepsilon)$, is used [12–14]:

$$\xi_{ab}(\varepsilon) = \xi_{ab}(0)\varepsilon_G^{1/6}\varepsilon^{-2/3}. \quad (8)$$

Finally, in the case of $\Delta\sigma_{ab}^i(\varepsilon)$ and still closer to the transition, a full dynamic scaling theory [12, 14, 21] predicts a critical exponent in (8) of $-1/3$.

The full lines in figure 2(a) and (b) correspond to the best fit of, respectively, (4) and (5) in the indicated MFR and with A_{AL} , A_S and B_{LD} (in the two curves) as free parameters. The resulting values are $A_{AL} = (380 \pm 70) (\Omega \text{ cm})^{-1}$; $A_S = (6 \pm 2) \times 10^{-10} \text{ K}^{-1}$ and $B_{LD} = 0.13 \pm 0.06$ (this last value being the same for the two curves). Concerning these A_{AL} and B_{LD} values, let us remark that:

(i) The indicated uncertainties are associated with the dispersion of the data analysed here. If we also take into account the background dispersion (see above) the values extracted from $\Delta\sigma_{ab}^i$ are $A_{AL} = (350 \pm 100) (\Omega \text{ cm})^{-1}$ and $B_{LD} = 0.15 \pm 0.05$.

(ii) The difference from the values proposed in [2], $A_{AL} = (310 \pm 50) (\Omega \text{ cm})^{-1}$ and $B_{LD} = 0.16 \pm 0.05$, are due (mainly) to the fact that in the present work we have neglected any 'anomalous' (Maki-Thompson) contribution to $\Delta\sigma_{ab}^i(\varepsilon)$ and also to the use of a linear T -dependence for the background. These values lead directly to the intrinsic $\text{Y}_1\text{Ba}_2\text{Cu}_3\text{O}_{7-\delta}$ characteristic lengths (in \AA): $\xi_{ab}(0) = (9 \pm 2)\sqrt{n}$; $d_c = (4 \pm 1)n$, and $\xi_{\perp}(0) = (0.7 \pm 0.2)n$. For $n = 2$, these values of $\xi_{\perp}(0)$ and $\xi_{ab}(0)$ are well inside the different proposals in the literature [22]. The corresponding Lawrence-Doniach effective length, $d_c = (8 \pm 2) \text{\AA}$, is close to the largest distance between adjacent CuO_2 planes in these compounds (8.3\AA). This agreement between our experimental results and the conventional SCOPF theories seems to be confirmed in the crossover region, beyond the MFR. The broken lines in figure 2(a) and (b) correspond to, respectively, (6) and (7) with $\xi_{ab}(\varepsilon)$ given by (8). The $\xi_{ab}(0)$ and $\xi_{\perp}(0)$ values used now are those obtained in the MFR (with $n = 2$) and for ε_G we have used the average lower ε -limit of the MFR: $\varepsilon_G = 0.7 \times 10^{-2}$. As it is clearly observable in these figures, the agreement, found without any free parameter, is excellent. In the case of $\Delta\sigma_{ab}^i(\varepsilon)$, where we may resolve up to $\varepsilon \geq 10^{-4}$, our present experiments confirm the existence of a different ε -behaviour for $\varepsilon \leq 10^{-3}$ that perhaps may be associated with the full critical regime, as first suggested in [23]. However, as it was also suggested then and as recent analysis confirms quantitatively [24], the influence of various types of inhomogeneities may be important that close to the transition. Let us just note, finally, that the behaviour of both observables for $\varepsilon \geq 0.1$ may be attributed tentatively to the simultaneous presence of a low dimensionality LD-like crossovers and a non-mean field regime. We must stress, however, that the uncertainties associated with the background are relatively important in this reduced temperature region.

In conclusion, we have reported high-resolution data of the electrical resistivity and of the magnetic susceptibility rounding effects above the superconducting transition obtained in the same single-phase polycrystalline $\text{YBa}_2\text{Cu}_3\text{O}_{7-\delta}$ samples. The temperature resolutions were 10 mK for $\rho(T)$ and 0.1 K for $\chi(T)$, the last improving previous $\chi(T)$ measurements by an order of magnitude. In this way we have probably been able to penetrate, for the first time in the case of $\chi(T)$, beyond the mean-field region closer to the transition. The data in the MFR and in the crossover region have been explained quantitatively and consistently in terms of the existing theoretical approaches based on *direct* thermodynamic fluctuations in 3D of the amplitude of a two-component order parameter for unconventional superconductors. The absence of appreciable pair-breaking effects on $\Delta\sigma_{ab}^i(\varepsilon)$ is, therefore, confirmed [2]. The resulting intrinsic parameters are: $A_{AL} = (350 \pm 100) (\Omega \text{ cm})^{-1}$, $A_S = (6 \pm 2) \times 10^{-10} \text{ K}^{-1}$, $B_{LD} = (0.15 \pm 0.08)$ and $\varepsilon_G = (0.7 \pm 0.3) \times 10^{-2}$. The corresponding intrinsic characteristic lengths amplitudes are $\xi_{ab}(0) = (12 \pm 3) \text{\AA}$, $\xi_{\perp}(0) = (1.4 \pm 0.4) \text{\AA}$, and $d_c = (8 \pm 2) \text{\AA}$.

We acknowledge E Morán and A Várez for providing us with the high-quality YBCO samples. This work has been supported by the CICYT (MAT 88-0769), the Programa MIDAS (89-3800) and the Fundación Ramón Areces, Spain.

References

- [1] Veira J A and Vidal F 1989 *Physica C* **159** 468 and references therein
- [2] Veira J A and Vidal F 1990 *Phys. Rev. B* **42** 8748 and references therein
- [3] Friedmann T A *et al* 1989 *Phys. Rev. B* **39** 12264
- [4] Hikita M and Suzuki M 1990 *Phys. Rev. B* **41** 834 and references therein
- [5] Kanoda K *et al* 1988 *J. Phys. Soc. Japan* **57** 1554
Kawagoe T *et al* 1988 *J. Phys. Soc. Japan* **57** 2272 and references therein
- [6] Lee W C, Klemm R A and Johnston D C 1989 *Phys. Rev. Lett.* **63** 1012
- [7] Lee W C and Johnston D C 1990 *Phys. Rev. B* **41** 1904 and references therein
- [8] Lawrence J and Doniach S 1971 *Proc. 12th Int. Conf. on Low Temperature Physics (Kyoto, 1970)*
ed E Kanda (Tokyo: Academic) p 361
- [9] Aslamazov L G and Larkin H I 1968 *Phys. Lett. A* **26** 238
- [10] Schmidt H 1968 *Phys. Lett. A* **27** 658
- [11] Skocpol W J and Tinkham M 1975 *Rep. Prog. Phys.* **38** 1049
- [12] Lobb C J 1987 *Phys. Rev. B* **36** 3930
- [13] Kulić M L and Stenschke H 1988 *Solid State Commun.* **66** 497
- [14] Bulaevskii L N, Ginzburg V L and Sobyenin A A 1988 *Physica C* **152** 378
- [15] Weigang G and Winzer K 1989 *Z. Phys.* **B 77** 11
- [16] Friedmann T A, Rice J P, Gianpirtzakis J and Ginsberg D M 1990 *Phys. Rev. B* **42** 6217
- [17] Hagen S J, Jing T W, Wang Z Z, Horvath J and Ong N P 1988 *Phys. Rev. B* **37** 7928
- [18] See for instance,
Vidal F 1982 *Phys. Rev. B* **26** 3986 and references therein
- [19] Yip S K 1990 *Phys. Rev. B* **41** 2012; 1990 *J. Low. Temp. Phys.* **81** 129
- [20] Klemm R A 1990 *Phys. Rev. B* **41** 2073
- [21] Hohenberg P C and Halperin B I 1977 *Rev. Mod. Phys.* **49** 435
- [22] See for instance,
Krusin-Elbaum L *et al* 1989 *Phys. Rev. B* **39** 2936
Welp U *et al* 1989 *Physica C* **162-164** 735
- [23] Veira A, Maza J and Vidal F 1988 *Phys. Lett. A* **131** 310
- [24] Maza J and Vidal F 1991 *Phys. Rev. B* at press